Research in Astron. Astrophys. **2012** Vol. **12** No. **8**, 865–890
http://www.raa-journal.org *http://www.iop.org/journals/raa*

***R**esearch in*
***A**stronomy and*
***A**strophysics*

Observations of the first light and the epoch of reionization

Xiaohui Fan

Kavli Institute for Astronomy and Astrophysics, Peking University, Beijing 100871, China; Steward Observatory, The University of Arizona, Tucson, 85721, USA; *fan@as.arizona.edu*

Received 2012 July 10; accepted 2012 July 14

Abstract Studying the first generation of stars, galaxies and supermassive black holes as well as the epoch of reionization is one of the fundamental questions of modern astrophysics. The last few years have witnessed the first confirmation of the discoveries of galaxies, quasars and Gamma-Ray Bursts at $z > 7$, with possible detections at $z \sim 10$. There is also mounting evidence that cosmic reionization is a prolonged process that peaks around $z \sim 10$ and ends at $z \sim 6 - 7$. Observations of the highest redshift intergalactic medium and the most metal-poor stars in the Galaxy begin to constrain the earliest chemical enrichment processes in the Universe. These observations provide a glimpse of cosmic history over the first billion years after the Big Bang. In this review, we will present recent results on the observations of the high-redshift Universe over the past decade, highlight key challenges and uncertainties in these observations, and preview what is possible with the next generation facilities in studying the first light and mapping the history of reionization.

Key words: galaxies: evolution — galaxies: formation — galaxies: high-redshift — intergalactic medium — quasars: general — cosmology: large-scale structure of universe

1 INTRODUCTION

After the recombination epoch at $z \sim 1200$ (Komatsu et al. 2011), the intergalactic medium became mostly neutral, while astronomical objects — stars, galaxies, quasars — had yet to be formed from gravitational collapse. The Universe entered the "cosmic dark ages" (Rees 1998). At $z \sim 20 - 50$, the first generation of dark matter halos with $\sim 10^6\ M_\odot$ formed in the Universe. Baryons in these haloes would first collapse to higher density through radiative cooling of molecular hydrogen and the very first generation of stars began to form in these systems. The first generation, or Population-III, stars were metal-free and are thought to be much more massive than current generation stars, with a characteristic mass of 30 – 100 $M_\odot$ (e.g. Abel et al. 2002; Yoshida et al. 2006). The formation of the first stars has important consequences: firstly, they are powerful emitters of energetic UV photons and provide important radiative feedback by ionizing the surrounding interstellar medium (ISM) and eventually the still-largely-neutral intergalactic medium (IGM); secondly, during the post main sequence phase of these short-lived stars, they eject kinetic energy as well as heavy elements into the surrounding ISM, first through stellar wind, and eventually by supernova explosion. Finally, over a wide range of stellar masses, these massive stars will collapse to form the first stellar mass black holes, which would become the seeds of the first generation active galactic nuclei (AGNs) and grow into the first supermassive black holes and quasars. Furthermore, the UV photons from the first

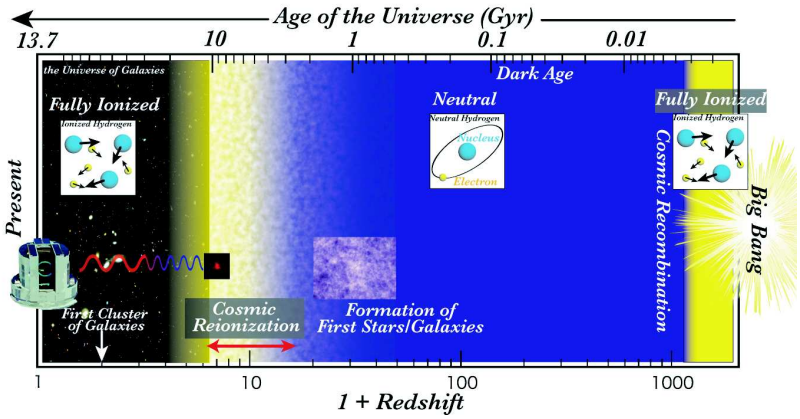

Fig. 1 Cosmic history and landmark events since the epoch of recombination. The formation of the first generation of stars and galaxies is expected to have happened at redshift $z > 20$, while the epoch of reionization is at $z = 6 - 15$, marking the end of the cosmic dark ages. Image credit: National Astronomical Observatory of Japan (*http://www.naoj.org/Pressrelease/2012/06/03/index.html*).

generation of galaxies and quasars ionized the neutral hydrogen in the IGM, resulting in the *cosmic reionization* at redshift of ~ 10 (e.g., Dunkley et al. 2009), ending the cosmic dark ages.

Figure 1 illustrates the timeline of the first one billion years of cosmic history. First light and reionization are landmark events of cosmic evolution. They are also one of the remaining frontiers in our understanding of cosmic history and a focus of intense observational and theoretical investigations on both fronts, making it a fast-moving field. However, even with tremendous progress in the last decade, some of the basic questions remain unanswered or poorly understood:

– When did the first stars and first galaxies form? What were their masses?
– When did the first supermassive black holes form, and how did the growth of supermassive black holes and galaxies affect each other at the early epoch?
– How did the first generation of objects affect the ISM and IGM through radiative, kinetic and chemical feedback? When did the first metals propagate into the IGM?
– When was the epoch of reionization? Was it a gradual and prolonged process or a sharp phase transition? What were the sources of reionization?

The purpose of this review is to give a relatively brief update on the observational studies of the highest redshift galaxies and quasars, focusing on searching for the first galaxies and first supermassive black holes, and the observational constraints on cosmic reionization. There are many excellent reviews on this subject. For comprehensive reviews, the readers are referred to the recent book by Loeb (2010), and the articles from the Annual Review of Astronomy and Astrophysics in the last decade or so by Bromm & Yoshida (2011); Morales & Wyithe (2010); Fan et al. (2006a); Bromm & Larson (2004); Loeb & Barkana (2001).

Observationally, studying first light means searching for the most distant galaxies and quasars. Figure 2 summarizes the history of discovery for the most distant galaxies, quasars and Gamma-Ray Bursts (GRBs) with secure spectroscopic confirmations. This has always been one of the most challenging and demanding tasks of observational astronomy as it constantly puts the technical capability and available observing resources to the limit. The last few years have finally witnessed the discovery of galaxies, quasars and GRBs at $z > 7$, within the first Gyr of cosmic history and close to, or even within, the epoch of reionization. In Section 2 and Section 3, we will review the basic tech-

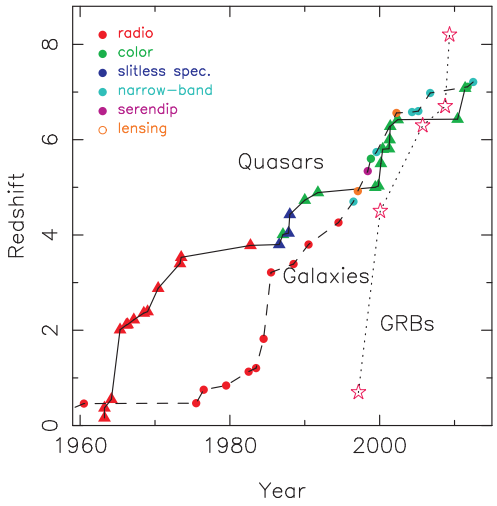

Fig. 2 Record of the highest-redshift spectroscopically-confirmed galaxies, quasars and Gamma-Ray Bursts as a function of time.

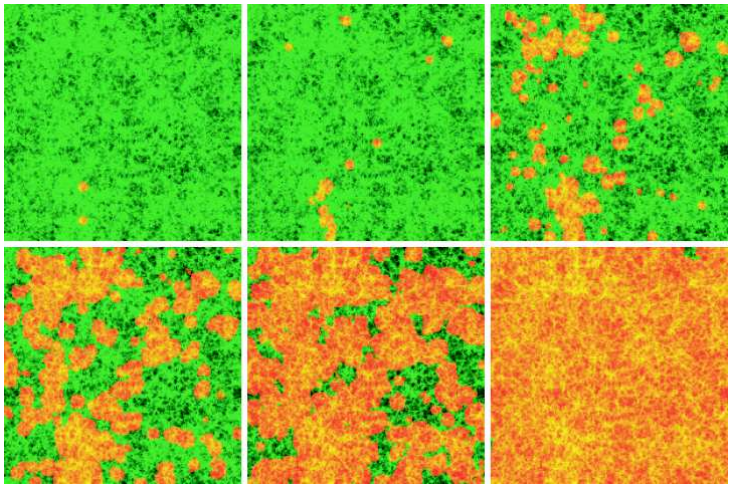

Fig. 3 Reionization Simulation on the scale of 100 Mpc. Slices through the simulation volume are at redshifts $z = 18.5$, 16.1, 14.5, 13.6, 12.6 and 11.3. The density field (*green* in neutral regions, *yellow* in ionized regions) and the HII regions (*red*) are both shown. Adapted from Iliev et al. (2006).

niques of high-redshift galaxy and quasar surveys, and our current understanding of their physical properties. We will discuss observations of first metals in the IGM and the use of most metal-poor stars in the Milky Way as probes of first light in Section 4.

Theoretical modeling of the reionization process (Fig. 3) has proven to be challenging: it requires detailed simulations of not only the large scale cosmological structure, but also small scale baryonic processes and radiative transfer processes that affect the ionization state of the gas at all scales. Observationally, the lack of complete Gunn-Peterson (Gunn & Peterson 1965) absorption at

$z < 6$ indicates that the IGM is highly ionized by that epoch (e.g., Becker et al. 2001; Djorgovski et al. 2001). At the other end of the reionization history, polarization measurements of the cosmic microwave background (CMB) from WMAP (e.g., Dunkley et al. 2009) show a large optical depth due to Thompson scattering of electrons in the early Universe, suggesting that the IGM was largely ionized by $z \sim 10.6 \pm 1.2$. However, a detailed history of reionization remains largely uncertain beyond these two crude constraints. In Section 5, we will review the current observational constraints on the history of reionization, which strongly suggest a prolonged, gradual process.

The current highest redshift frontier is at $z \geq 7$. However, this is not yet when the first generation of galaxies formed; the bulk of reionization activities is also thought to be at earlier epochs. Pushing to higher redshift to unveil the epoch of the first light requires more powerful next generation facilities both on the ground and in space. We close by discussing some of the future prospects in Section 6.

2 FIRST GALAXIES

Searches for the highest redshift galaxies are completely driven by our technical ability to carry out deep imaging and spectroscopic observations towards increasingly longer wavelengths. Observations of the first billion years ($z > 6$) only opened up in the last decade or so, with the advent of relatively wide-field, deep imaging observations using the largest ground-based 8–10 m class telescopes and HST for imaging selection, and the ability to carry out deep far-optical and near-IR spectroscopic confirmation. A large number of selection methods have been used to select photometric samples of high-redshift galaxies; however, spectroscopic confirmation of these candidates remains extremely challenging. Our understanding of the statistical properties of the $z > 6$ galaxy population has been rapidly improving; detailed studies of their physical properties are just beginning and are limited to the brightest sources at this redshift. A very comprehensive recent review of this subject is given in Dunlop (2012).

2.1 Surveys of High-redshift Galaxies

2.1.1 Lyman break galaxies (LBGs)

The most commonly used method of selecting high-redshift galaxies as well as high-redshift quasars is the Lyman Break technique: a galaxy's spectrum is significantly absorbed by neutral hydrogen in both its own ISM and the intervening IGM at wavelengths shorter than Lyα, which redshifts into the optical wavelength at $z > 3$. Therefore high-redshift objects would appear to have red color and drop out in the bluer bands that are affected by the Lyman Break. This selection technique only requires broad-band photometry, therefore it can be applied to wide-field surveys both on the ground and from space, and is able to reach low continuum luminosity. It was applied in wide-field $z > 4$ quasar surveys in the 1980s (Warren et al. 1987) and revolutionized the studies of high-redshift galaxies by the works of Steidel and collaborators (e.g. Steidel et al. 1996). As the Lyman Break redshifts towards a longer and longer wavelength, red and eventually near-IR imaging is needed to select galaxies at $z > 5$. For the highest redshift at $z \geq 7$, the HST deep fields have proven to be the most powerful resource for discovery, especially after the successful deployment of the infrared channel of its Wide-Field Camera 3 (WFC3). Thousands of LBGs have been selected through photometric selection at $z > 5$, with a handful of highly likely detections at redshift as high as $z \sim 10$ (Bouwens et al. 2011a). The new HST Multi-Cycle Treasure Program CANDELS (Grogin et al. 2011; Koekemoer et al. 2011) is utilizing the ACS and WFC3/IR instruments on the HST, aiming at studying the evolution of LBGs from $z = 1.5$ up to $z = 8$ with a sample of more than 250 000 galaxies, and is able to reach stellar mass as low as $10^9\, M_\odot$. LBG surveys are also carried out through deep ground-based imaging, which usually cover significantly larger areas than HST is able to, therefore discovering the most luminous LBGs. For example, Bowler et al. (2012)

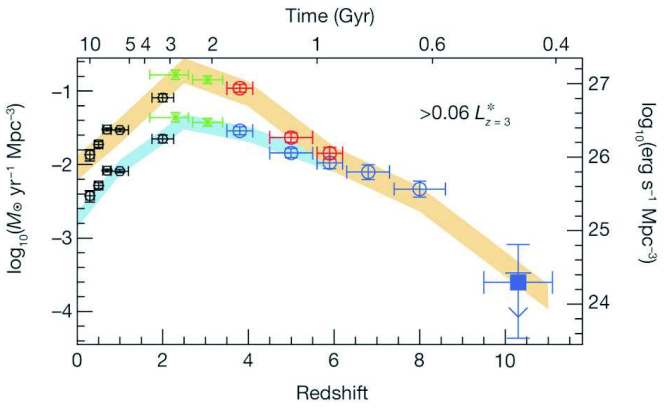

Fig. 4 The rest-frame continuum UV luminosity density (*right axis*) at $z \sim 10$, and the star formation rate density (*left axis*) derived from the extinction-corrected luminosity density. The comoving star formation density in the Universe has a broad peak at $z = 2 - 5$ and appears to be declining towards higher redshift at the end of the reionization epoch. Adapted from Bouwens et al. (2011a).

conducted a survey of 1 deg^2, reaching a continuum level of 25 mag AB, and selected a sample of ~ 10 highly luminous galaxies at $z > 6.5$.

A key result from LBG surveys is the determination of the overall star formation history over cosmic time, since the observed rest-frame UV luminosity directly traces the unobscured star formation rate.

Figure 4 shows the most recent compilation by Bouwens et al. (2011a) using a number of HST deep field observations, after correcting for extinction in high-redshift galaxies. The star formation density peaks at $z = 2 - 5$, and begins to evolve modestly towards high redshift. This evolution appears to accelerate at $z > 6$, indicating that we are closing in on the epoch of initial build-up of galaxy populations close to the reionization epoch.

Confirming LBGs spectroscopically at high redshift, however, has proven to be challenging for the current generation of telescopes. Contaminants from either low-redshift galaxies where the Lyman Break is confused with the 4000 Å break, or red galactic objects (e.g. L and T dwarfs), require spectroscopic follow-up to positively identify their redshift. At $z > 6 - 7$, continuum detection is nearly impossible with ground-based spectroscopy; redshift determination is based on Lyα emission line detection, often at low S/N level and relies critically on the accurate removal of very strong atmospheric OH lines. There have been examples of highly controversial spectroscopic confirmations over the years. The highest redshift LBGs with secure redshift is currently at $z = 7.1$ (Vanzella et al. 2011).

2.1.2 Lyα emitters

The nebula Lyα emission line is the strongest emission line in the rest-frame UV from young star forming galaxies. At $z > 5$, it often has high equivalent width (rest-frame > 30 Å up to ~ 200 Å), and therefore can represent a significant flux enhancement when galaxies are observed with narrow-band filters centered at the expected Lyα wavelength. Lyα searches are usually conducted in a few clean wavelength windows ($\sim$ 100 – 300 Å) with a much reduced level of OH emission from the atmosphere, allowing the ground-based survey to reach a very faint flux level as a result of lower sky background. Commonly used windows correspond to Lyα redshifts of $z = 4.5, 5.7, 6.5$ (e.g., Hu et al. 2002; Rhoads et al. 2003; Taniguchi et al. 2010). In recent years, deep-depletion CCD

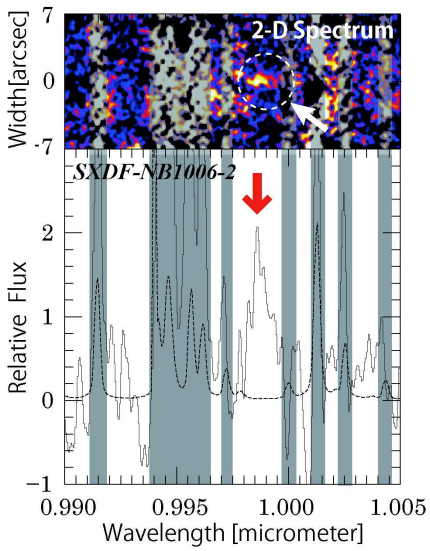

Fig. 5 The highest-redshift spectroscopically confirmed galaxy at $z = 7.22$. The figure shows the one- and two- dimensional spectra of SXDF-NB1006-2 obtained with the spectrograph DEIMOS on the Keck Telescope. The asymmetric emission line profile strongly suggests that the line is Lyα at $z = 7.22$. Adapted from Shibuya et al. (2012).

detectors have enabled efficient observations at $\lambda \sim 1$ μm, and opened up the atmospheric windows corresponding to $z = 7.0$ and 7.3 (Iye et al. 2006; Ota et al. 2008; Iye 2008). There have also been attempts to utilize windows in the J-band at higher redshift (e.g., Cuby et al. 2007; Clément et al. 2012) but such surveys have proven to be challenging. A major advantage of the Lyα survey is that it has selected objects with strong emission lines in relatively clean atmospheric windows, therefore greatly reducing the difficulty of spectroscopic confirmation.

Surveys of Lyα emitters have proven to be an extremely effective way of studying the high-redshift Universe, especially with a series of successful projects using the prime focus camera on the 8.2m Subaru telescopes (e.g., Kashikawa et al. 2006; Ouchi et al. 2010). The majority of galaxies at $z > 6.5$ with spectroscopic confirmation are selected with this technique, with the current highest redshift at $z = 7.22$ (Fig. 5, Shibuya et al. 2012). Because Lyα emitter surveys only focus on objects with strong Lyα emission lines, there is a possible bias between the Lyα galaxy population and LBG population, which is regarded to be more representative because it is selected on the basis of continuum luminosity. Radiative transfer of Lyα photons is a key to understanding the nature of Lyα galaxies (e.g., Zheng et al. 2010). On the other hand, Lyα detectability is also affected by IGM radiative transfer and provides a powerful way to probe the history of reionization (Sect. 5.2).

A major difficulty in studying the first galaxies is their faint flux level. If high-redshift galaxies are located behind a massive cluster of galaxies at an intermediate redshift, their flux could be magnified by a factor of a few to a few tens. Both LBG surveys and Lyα galaxy surveys have taken advantage of lensing in searching for the highest redshift galaxies. Hu et al. (2002) carried out narrow-band surveys of $z \sim 6.5$ Lyα galaxies. Stark et al. (2007) carried out a blind search of Lyα emitters by placing slits along critical lines in the lensing clusters, and discovered a number of candidates at $z > 7$. Another HST Multicycle Treasure program, CLASH (Postman et al. 2012), is conducting a deep multiband imaging survey of 25 massive clusters at $0.15 < z < 0.9$, with one of the main science goals of finding and characterizing the faint $z > 7$ population. Zheng et al. (2012)

discovered a highly magnified J-dropout object that is consistent with an LBG at $z \sim 9.6$ in the CLASH program.

2.1.3 Sub-millimeter galaxies

A complementary way of studying high-redshift galaxies is to observe their sub-millimeter radiation. Dust in the ISM of star forming galaxies absorbs UV radiation from young stars and re-emits it in the far-infrared and sub-millimeter wavelengths, forming a second peak in the galaxy's SED that contains a significant amount of its total bolometric luminosity. This far-infrared component has an effective temperature of $30 - 50\,\mathrm{K}$ and peaks at around $100\,\mu\mathrm{m}$; as galaxy redshift increases, sub-millimeter observations sample shorter rest-frame wavelengths close to this SED peak, resulting in a negative K-correction which largely compensates for the increasing luminosity distance. Therefore, galaxies at $z \sim 1 - 10$ have comparable apparent flux when observed in the far-infrared and sub-millimeter, making it a very effective wavelength to study high-redshift galaxies (e.g., Blain et al. 2000), although by observing dust emission, we by definition will not detect the first generation of galaxies that formed in a metal-free environment.

Another advantage of observing young galaxies in sub-millimeter is that this range is not affected by dust extinction in star forming regions. In addition, strong atomic and molecular lines in sub-millimeter and radio wavelengths, such as [CII] and CO, will enable redshift measurements completely independent from optical/near-IR spectroscopy. A number of high-redshift galaxies have been observed at $z > 5$ (e.g., Riechers et al. 2010), some without an optical counterpart and are based on a "blind" radio line search (e.g., Walter et al. 2012). The Atacama Millimeter Array (ALMA), with its transformational capability in sub-millimeter observations, will open a new window into studies of the earliest galaxies in the Universe.

2.1.4 Gamma-Ray bursts

Gamma-Ray Bursts (GRBs) are the most powerful explosions in the Universe, and could be detected at $z > 10$. At high-redshift, the time dilation means that their afterglow will fade away $(1 + z)$ times slower, aiding rapid spectroscopic follow-up observations (e.g Ciardi & Loeb 2000). Long-duration GRBs are thought to have originated from the collapse of massive stars, therefore the evolution of GRBs over cosmic time provides a complementary way to provide star formation rates in the Universe (e.g. Robertson & Ellis 2012). If caught early on, their near-IR afterglows would still be bright enough to provide a powerful probe of the evolution of the surrounding ISM in the GRB host galaxies and intervening IGM. The launching of the SWIFT satellite (Gehrels et al. 2004) revolutionized GRB afterglow studies. As shown in Figure 2, within a few years, the highest redshift GRBs have been detected at redshift as high as $z = 8.2$ (Salvaterra et al. 2009; Tanvir et al. 2009, Fig. 6) with spectroscopic follow-up, and at $z \sim 9.4$ (Cucchiara et al. 2011) with photometric selections.

2.2 High-redshift Galaxies as the Sources of Reionization

Regardless of the detailed reionization history (Sect. 5), the IGM has been almost fully ionized since at least $z \sim 6$. This places a minimum requirement on the emissivity of UV ionizing photons per unit of comoving volume required to keep up with recombination and maintaining reionization (Miralda-Escudé et al. 2000)

$$\dot{\mathcal{N}}_{\mathrm{ion}}(z) = 10^{51.2}\,\mathrm{s}^{-1}\,\mathrm{Mpc}^{-3}\left(\frac{C}{30}\right) \times \left(\frac{1+z}{6}\right)^{3}\left(\frac{\Omega_b h^2}{0.02}\right)^{2}, \tag{1}$$

where $C \equiv \frac{\langle n_{\mathrm{H}}^2 \rangle}{\langle n_{\mathrm{H}} \rangle^2}$ is the clumping factor of the IGM.

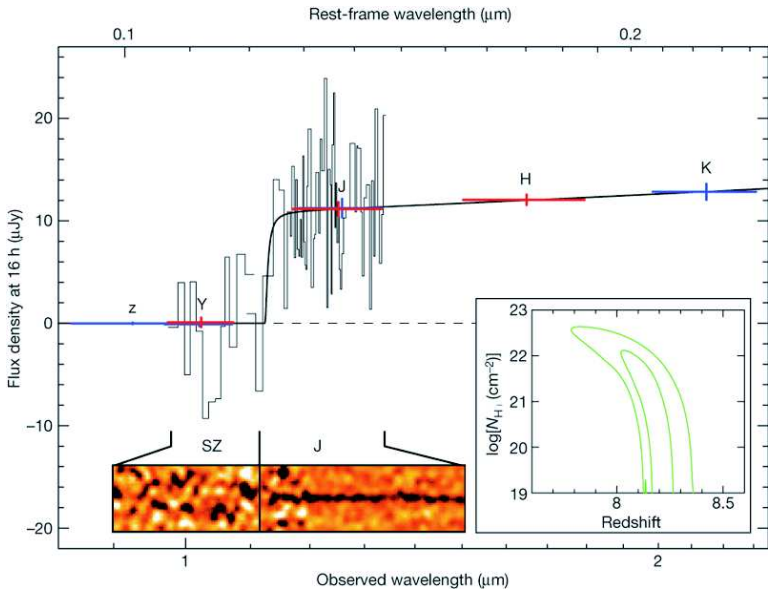

Fig. 6 The highest-redshift spectroscopically confirmed GRB at $z = 8.2$. Both broadband photometry and the sharp break in the afterglow spectra indicate that it is at $z > 8$. Adapted from Tanvir et al. (2009).

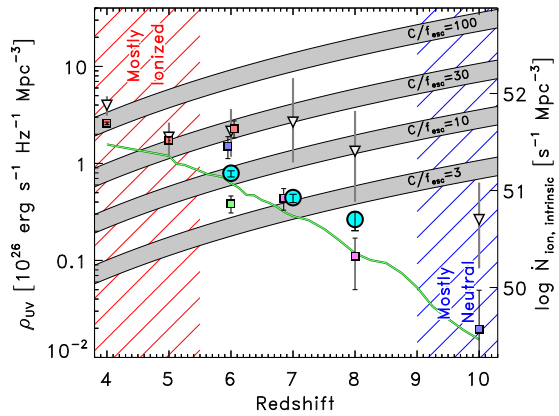

Fig. 7 The *observed* specific luminosity density (ρ_{UV}) versus redshift. The wide gray curves denote the value of ρ_{UV} needed to sustain a fully reionized IGM at a given redshift, for a given ratio of the clumping factor C over the escape fraction of ionizing photons $f_{\rm esc}$. The width of these curves represents changing stellar metallicities, from $0.02 < Z/Z_{\odot} < 1.0$. The right-hand vertical axis shows the corresponding intrinsic number density (i.e., prior to escape) of ionizing photons for a given specific UV luminosity density, using the median of a range of ages and metallicities, and assuming a constant star-formation history. The green curve shows the predicted luminosity density for sources brighter than $M_{1500} = -18$ from the hydrodynamic simulations of Finlator et al. (2011). Adapted from Finkelstein et al. (2012).

Due to the rapid decline in the AGN populations at very high z, most models assume stellar sources reionized the Universe. Robertson et al. (2010) summarizes the current status in locating galaxies responsible for cosmic reionization.

Figure 4 shows the present constraints on the evolution of UV luminosity and star formation rate of Lyman Break galaxies (Bouwens et al. 2011a). Compared to AGNs, the galaxy populations show less evolution at $z > 5$. However, despite rapid progress, there is still considerable uncertainty in estimating the total UV photon emissivity of star-forming galaxies at high-redshift. The uncertainties come from three factors: the star formation rate, clumping factor, and UV escape factor.

Determining the total star formation rate requires detailed measurement of the luminosity function for high-redshift galaxies. The faint end slope of the UV luminosity function of $z > 6$ galaxies is still poorly determined, with the index of the power law ranging from $\alpha = 1.5$ to 2.0 (e.g. Bunker et al. 2004, Yan & Windhorst 2004). New surveys using HST/WFC3 are able to reach considerably fainter luminosity at this redshift; more recent measurements appear to favor a steep faint-end slope (e.g. Bouwens et al. 2011b), although still with large uncertainty. Finkelstein et al. (2012, Fig. 7) present the most recent measurement of galaxy counts at $6 < z < 8$ based on deep observations over the CANDELS field, and found that by counting the *observed* galaxies in their survey, an escape fraction of $\sim 30\%$ is needed to sustain a fully-ionized IGM at $z \sim 6$, while the currently detected population will not be able to maintain reionization at $z > 7$.

Determination of the escape fraction remains a key challenge. Steidel et al. (2001) inferred a relatively large escape fraction based on a composite spectrum of 29 Lyman Break Galaxies. Shapley et al. (2006) presented the first direct detection of the Lyman continuum from Lyman Break Galaxies, indicating a lower escape fraction. The measurement, however, is only based on two detections. Siana et al. (2007) presented deep far-UV imaging of sub-L^* galaxies at $z \sim 1.3$, showing no detection of the Lyman continuum photons among 21 galaxies observed with HST. If this is true, Gnedin (2008) argued that there might not be enough UV photons from dwarf galaxies to reionize the Universe by $z > 6$. Given these uncertainties, the current data are consistent with star forming galaxies, in particular, relatively low luminosity galaxies, as being the dominant sources of reionizing photons, although more exotic sources, such as high-redshift mini-quasars, cannot yet be ruled out as minor contributors to the reionization budget.

3 FIRST SUPERMASSIVE BLACK HOLES

Discoveries of luminous quasars at $z > 6 - 7$ show that active, massive black holes of the order a billion solar masses existed a few hundred million years after the first star formation in the Universe, at the end of the reionization epoch. How does the black hole population grow with cosmic time? How does the evolution of quasar density trace the accretion history of early supermassive black holes? Locally, the tight correlation between the mass of central BHs and the velocity dispersion of host galaxies implies that black hole activity and galaxy formation are strongly coupled. How are the formation of galaxies and black hole activity related at early epochs?

As of summer 2012, 33 quasars have been discovered at $z > 6$, ~ 70 at $z > 5.5$, and over 100 at $z > 5$. Most of them were discovered using data from wide-field multicolor imaging surveys such as the Sloan Digital Sky Survey (SDSS, e.g., Fan et al. 2006c; Jiang et al. 2009), the Canadian-French High-z Quasar Survey (CFHQS, e.g., Willott et al. 2010a) and the UKIDSS Infrared Deep Sky Survey (UKIDSS, e.g, Mortlock et al. 2009). Currently, the highest redshift quasars are at $z = 7.09$, discovered in UKIDSS (Mortlock et al. 2011).

Figure 8 presents the spectra of all 33 published quasars at $z > 6$. Two features stand out immediately: there is strong redshift evolution of the transmission of the IGM: transmitted flux is clearly detected in the spectra of quasars at $z < 6$ and blueward of the Lyα emission line; the absorption troughs deepen for the high-redshift quasars, and complete Gunn-Peterson absorption begins to appear along lines of sight at $z > 6.1$. We will discuss this in detail in Section 5. On the

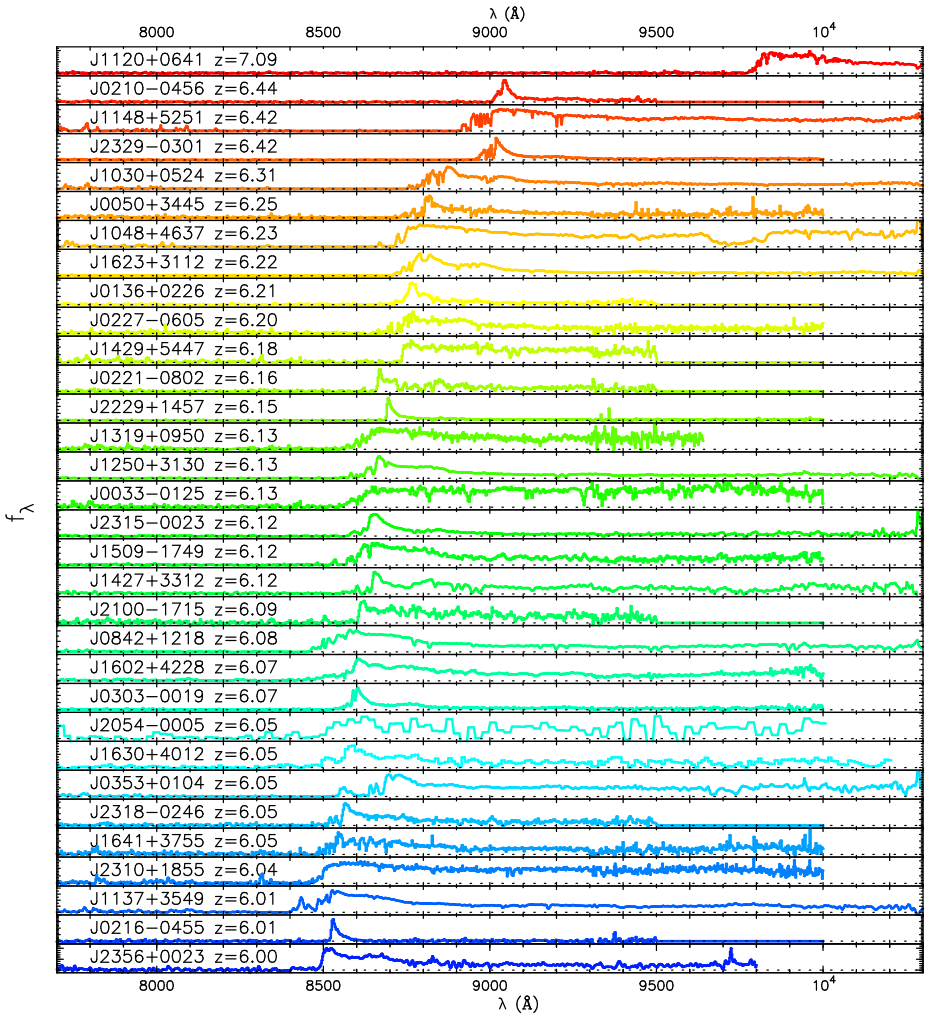

Fig. 8 Moderate dispersion spectra of all published quasars at $z > 6$ as of 2012 June. Note the strong Lyα absorption blueward of Lyα emission, especially the presence of complete Gunn-Peterson troughs at $z > 6.1$ at the end of the reionization epoch, and the existence of strong metal emission lines in the spectra, indicative of super-solar metallicity in the quasar environments. Adapted from Fan et al. (2004).

other hand, redward of Lyα emission, the spectra show clear detection of metal emission lines such as NV, SiIV (and CIV, MgII and FeII features in near-IR spectroscopy). Rapid chemical enrichment has occurred in the vicinity of these luminous quasars.

The density of luminous quasars is a strong function of redshift: it peaks at $z \sim 2-3$ and declines exponentially towards lower and higher redshifts (e.g. Boyle et al. 2000; Schmidt et al. 1995). Compared to the evolution of star-formation rate in the Universe, the quasar density peaks at higher redshifts, and evolves much faster. This exponential decline continues to the highest redshifts.

Figure 9 (based on Fan et al. 2004) presents the density of quasars at $M_{1450} < -26.7$ found in 6000 deg^2 of SDSS data at $z \sim 6$, along with the results from lower redshift (Fan et al. 2001). The

quasar density at $z \sim 6$ found here is consistent with extrapolating the best-fit quasar luminosity functions in the range $3 < z < 5$. The comoving density of luminous quasars at $z \sim 6$ is ~ 40 times smaller than that at $z \sim 3$, as we approach the epoch of formation of the first supermassive black holes in the Universe.

The existence of these objects is an amazing feat in the process of galaxy formation and challenges models of black hole formation. The SDSS $z \sim 6$ quasars are among the most luminous quasars at any redshift; their apparent magnitudes are ~ 19 even at $z > 6$! They are likely powered by supermassive black holes with several billion solar masses, and reside in the dark matter halo of $10^{13} M_{\odot}$. They are among the most massive black holes and galaxies at any redshifts. How could the universe have formed with such massive galaxies, and in particular, have assembled such massive black holes in the first Gyr of cosmic evolution? They are clearly the rarest and most biased systems in the early Universe, and probably started the initial assemblage at a redshift much higher than 10, well into the dark ages, providing important clues to the co-formation and co-evolution of the earliest supermassive black holes and galaxies.

The black hole mass estimates of the $z \sim 6-7$ SDSS quasars range from several times $10^8\ M_{\odot}$ to several times $10^9\ M_{\odot}$. In conventional models of supermassive black hole formation, they grow by a radiatively-efficient (with $\sim\ 10\%$ efficiency in converting gravitational potential energy to radiation), Eddington-limited accretion process, with an e-folding timescale of mass growth ~ 40 Myr. Indeed, most $z \sim 6-7$ quasars are found to be accreting close to the maximum Eddington rate (Willott et al. 2010b; De Rosa et al. 2011). Assuming continuous Eddington accretion from a seed black hole of 100 $M_{\odot}$, the formation redshift for seed black holes must be at $z > 10$. Even with continuous accretion, black holes in the most luminous quasars barely had enough time to grow. A number of models have been proposed to overcome this issue, either by direct formation of much more massive ($\sim 10^5\ M_{\odot}$) seed black holes, or by an early phase of super-Eddington accretion (e.g., Volonteri 2010). The fact that the highest redshift quasars sit right at the threshold of the reionization epoch simply indicates that the initial growth of those BHs had to be very efficient and very early.

Another challenge is the *lack of* evolution in the physical properties of luminous quasars, even as their density shows strong evolution. The average spectral energy distributions of luminous quasars in the rest-frame UV show little evolution out to high redshift (Fan et al. 2004); the intrinsic spectrum of the most distant quasar at $z = 7.09$ (Mortlock et al. 2011) is indistinguishable from that of a quasar in the local Universe. Using emission line ratios, it is shown that quasar broad emission line regions have roughly solar or even higher metallicities at $z \sim 6$ (e.g., Freudling et al. 2003; Jiang et al. 2007; De Rosa et al. 2011). This lack of evolution demonstrates that the emission line region and the accretion disk can form on a short timescale and are decoupled from the cosmological environment. These results put strong constraints on the enrichment history of quasar host galaxies and quasar environments as they grow to resemble the centers of current-day giant elliptical galaxies in less than one billion years.

Does this lack of high-energy SED evolution extend towards longer wavelengths? Much of the AGN emission is re-processed by the dust and gas in the host galaxy and re-emitted in IR wavelengths. This is the region where the AGN SEDs reach their peaks. In particular, have the properties of dust in the quasar environment, such as temperature and composition of dust and geometry of a dust torus, also been well established in such a short timescale? Jiang et al. (2010) carried out a survey of hot dust properties among $z \sim 6$ quasars using the Spitzer Space Telescope. They found that while most quasars show the presence of strong dust emission as in low-redshift quasars (e.g., lower panel, Fig. 10), two objects in the sample (upper panel, Fig. 10) are completely undetected with Spitzer to a faint limit. Prominent hot dust radiation, thought to be ubiquitous among type-1 quasars, is simply not there. Instead, their SEDs in the optical to mid-IR region are consistent with a pure accretion disk emission spectrum. No such object has been discovered at lower redshift. Furthermore, these two quasars have the smallest black hole mass, with the hot-dust abundance in the sample building up in tandem with the growth of the central black hole, whereas at low redshift

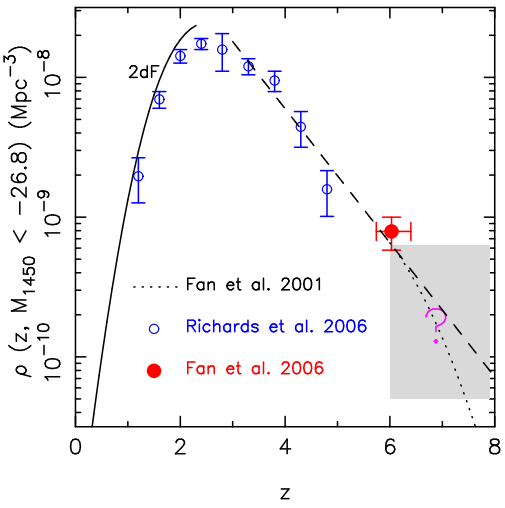

Fig. 9 Evolution of the density of luminous quasars based on the SDSS and 2dF surveys. Next generation near-IR surveys will extend these measurements to $z > 7$, and determine whether there is a sharp cutoff as we approach the epoch of the first billion $M_{\odot}$ BH formation.

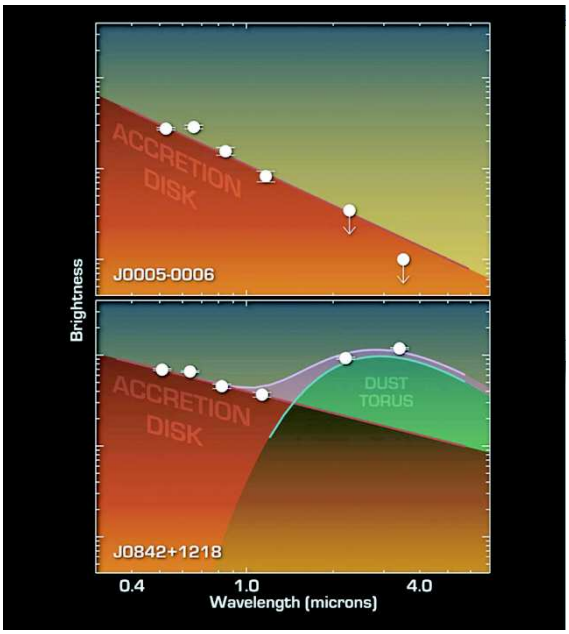

Fig. 10 The discovery of the first dust-free quasar at high redshift. The lower panel displays the SEDs of a normal quasar at $z \sim 6$, while the upper panel presents the SEDs of a dust-free quasar, which shows no detection of hot dust and is consistent with pure disk emission in the near to mid-IR. Adapted from Jiang et al. (2010).

it is almost independent of the black hole mass. Thus $z \sim 6$ quasars are indeed at an early evolutionary stage, with rapid mass accretion and dust formation. The two hot-dust-free quasars are likely to be first-generation quasars born in dust-free environments and are too young to have formed a detectable amount of hot dust around them.

Spectra of $z \sim 6$ quasars reveal strong metal emission lines from the surrounding gas. This suggests vigorous recent star formation in their host galaxies which enriched quasar environments. Luminous high-redshift quasars are likely located in the densest environments in the early Universe. However, direct imaging of the stellar light of host galaxies is extremely difficult for luminous high-redshift quasars. In observed far-IR to mm wavelengths, the radiation is dominated by the reprocessed radiation from cool/warm dust in the host galaxy, providing the best window to study host galaxy properties while minimizing contaminations from the quasar light. Millimeter and sub-millimeter continuum surveys of $z \sim 6$ quasars (e.g., Bertoldi et al. 2003; Wang et al. 2007, 2008) found that about 1/3 of high redshift quasars host galaxies that have luminosity comparable to those of hyper-luminous IR galaxies ($L_{\rm FIR} \sim 10^{13}\,L_{\odot}$). Assuming the dust heating came from starburst activity, this suggests an enormous star formation rate of $10^2 - 10^3\,M_{\odot}\,{\rm yr}^{-1}$. Quasar growth is accompanied by intense star formation.

Radio-line surveys of sub-millimeter-bright quasars at $z \sim 6$ detected strong CO emission in their host galaxies (e.g., Wang et al. 2010). The implied molecular gas masses are $\sim 10^{10}\,M_{\odot}$, and line widths range from 200 km s^{-1} to 800 km s^{-1}. Observations of gas dynamics in quasar host galaxies also provide the only way to study the M-σ or black hole - bulge mass relations at the highest redshift. CO imaging of a few $z \geq 4$ quasars shows a systematic departure from the low z relationship (Riechers et al. 2008, 2009; Walter et al. 2004). Wang et al. (2010) found that, assuming random inclination angles for the molecular gas, the $z \sim 6$ quasars are, on average, a factor 15 above the black hole – bulge mass relation, in the sense of over-massive black holes. This result suggests that BHs in high redshift quasars grow at a faster rate compared to the rate their host galaxies are being assembled; the M-σ relation, if it existed at $z \sim 6$, would show a strong cosmic evolution. Detailed sub-millimeter and radio observations of quasar host galaxies also provide evidence for quasar feedback on their hosts that could lead to the establishment of the M-σ relation. Maiolino et al. (2012) detected a broad wing in the [CII] line of a $z \sim 6.4$ quasar, suggesting strong outflow driven by the quasar which could quench the star formation activity of the entire galaxy. Recently, the [CII] line was detected in the highest redshift quasar at $z = 7.1$ (Venemans et al. 2012). Such observations will become routine and no longer be limited to the most luminous sources when ALMA reaches its full capability.

4 FIRST METALS AND FIRST STARS

The early star formation process that presumably started cosmic reionization also enriched the ISM and IGM with heavy elements. This is important as a chemical feedback mechanism, since the first metals in the ISM and IGM immediately affect the heating and cooling of gas and the subsequent star formation. Detailed metal enrichment models in the early universe are reviewed in Ciardi & Ferrara (2005). Becker et al. (2006, 2011) uncovered a number of low-ionization IGM metal absorption systems to redshift as high as $z \sim 6.2$, indicating an early IGM enrichment at the end of the reionization epoch. Systematic searches of CIV, usually the strongest IGM absorption line, have yielded detections of more than 20 IGM CIV systems at $z > 5$ (e.g., Simcoe et al. 2011; Ryan-Weber et al. 2009).

Figure 11 illustrates the evolution of IGM CIV mass density with redshift. The relative invariance in the amount of CIV absorption between $z \sim 2 - 5$ (Pettini et al. 2003; Songaila 2001) could imply that a significant amount of IGM metals was injected at $z > 5$. Schaye et al. (2003) found a lower bound of [C/H] ~ -4 even in the underdense regions of the IGM at $z < 4$. Meanwhile, CIV absorber surveys have convincingly demonstrated that there is a rapid evolution in the comoving

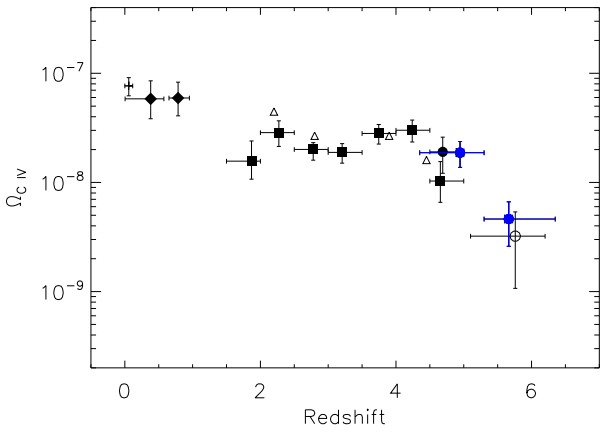

Fig. 11 Evolution of the mass density in CIV absorption in the intergalactic medium. There is a strong downturn at $z > 5$, indicating an evolution in either the Carbon enrichment or ionization state at this redshift. Adapted from Simcoe et al. (2011).

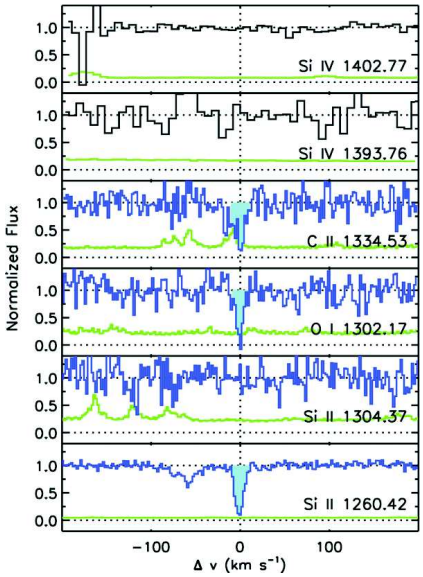

Fig. 12 The IGM metal absorption system with the highest known redshift at $z = 6.25$. Adapted from Becker et al. (2011).

number density of CIV absorbers, with a factor of ~ 5 decrease between $z = 5$ and 6 (e.g., Simcoe et al. 2011; Ryan-Weber et al. 2009).

IGM is evolving rapidly in a post-reionization Universe. What are the sources of early metals and how did they get there? Evolution of high-redshift galaxies critically relies on their ability to regulate their star formation with galactic superwind feedback. Dave et al. (2006) showed that simulations

without feedback build galaxies with mass and star formation rates at least three times too high. A fundamental prediction of the galactic superwind model is that they, at the same time, would enrich their surrounding IGM with heavy elements — they are the sources of early IGM enrichment. Adelberger et al. (2005) studied the IGM-galaxy connection at $z \sim 3$ based on a survey of galaxies associated with CIV absorption. Only one of the strongest CIV systems at $z > 5$ has an associated galaxy identified through ultra-deep ground-based Lyα spectroscopy (Gonzalo Diaz et al. 2011).

Madau et al. (2001) found that by assuming massive stars ionized the Universe with yield produced from Population II or III stars, the Universe would have a mean metallicity of $\sim 10^{-3} \sim 10^{-4} Z_\odot$ after reionization, comparable to those values found in the high-redshift quasar absorption lines. While these measurements do not directly constrain the reionization history, they suggest that one could detect numerous metal absorption lines even at $z > 6$. Furlanetto & Loeb (2003) suggest using observations of low-ionization absorption lines such as CII or OI to constrain properties of the stellar population that ionized the Universe at $z > 6$, such as star formation efficiency and escape fraction from supernova winds. To directly constrain the reionization history, Oh (2002) suggested using OIλ1302 absorption as a tracer of the neutral fraction. OI has almost identical ionization potentials as H and should be in a tight charge exchange equilibrium with H, while its lower abundance means that it would not saturate even when the Universe was mostly neutral: $\tau_{\rm OI}^{\rm eff} = 10^{-6} \left(\frac{\langle Z \rangle}{10^{-2} Z_\odot}\right) \tau_{\rm HI}^{\rm eff}$. OI (and SiII λ1260) forests could provide combined constraints on the reionization and metal enrichment histories. Oh (2002) predicted that a handful of OI lines could be detected in the Gunn-Peterson trough redshift regions of known $z > 6$ quasars when observed at high resolution.

Becker et al. (2006, 2011, Fig. 12) obtained high-resolution, high S/N spectra of a sample of six quasars at $z > 5$ using Keck/HERES and detected an OI system up to $z = 6.26$. They do not find a dense OI forest, consistent with a high degree of IGM ionization at $z \sim 6$. However, it is puzzling that the line of sight of SDSS J1148+5251 ($z = 6.42$), which has the highest ionization fraction at $z > 6$ (Sect. 3.3), also has the highest density of OI lines, raising the possibility that low metallicity, not high ionization, may be the cause for the lack of OI lines. Detailed modeling of IGM enrichment is needed to interpret results from high-redshift metal lines.

The first stars, i.e., Population III (Pop III) stars with zero metallicity, are likely to be very massive due to inefficient cooling and the large Jeans mass in the early universe (Abel et al. 2002; Yoshida et al. 2006). Massive Pop III stars are probably key contributors to both the ionization photons that caused cosmic reionization and to the early phases of cosmic chemical evolution (Whalen et al. 2008; Mackey et al. 2003; Bromm et al. 2003). Observations of the formation of individual Pop-III stars are probably beyond the reach of even JWST (Zackrisson 2012). Can we detect the combined contribution of Pop-III stars among high-redshift galaxies? There have been a number of such attempts that searched for the HeII $\lambda 1640$ emission lines, since they can arise from highly energetic ionizing photons associated with hot, metal-free stars. Dawson et al. (2004), Ouchi et al. (2008), and Nagao et al. (2005) searched for an HeII $\lambda 1640$ line in either stacked or individual spectra of Lyα-emitting galaxies, and their non-detections constrain the massive Pop III star formation rate to a few $M_\odot$ yr^{-1}, usually a few tenths of the overall SFR in these galaxies. The most stringent limit so far came from deep HST narrow-band observations of a $z = 6.96$ Lyα emitter centered on its expected HeII emission line (Cai et al. 2011), setting an upper limit on the Pop III star formation rate in this galaxy to be $< 0.5 M_\odot$ yr^{-1}, or $\sim 6\%$ of its on-going star formation at $z \sim 7$.

The other direction for probing the first generation of star formation is to study the most metal poor stars in the Galaxy. While Pop III stars are expected to be massive, they will quickly enrich the surrounding ISM with heavy elements, resulting in a critical metallicity (e.g., Bromm & Loeb 2003; Schneider et al. 2003) below which there is more efficient cooling and formation of low mass stars that could survive until the current epoch. Chemical abundances of these low-mass second generation stars bear signatures of the nucleosythesis and chemical enrichment processes of the first stars.

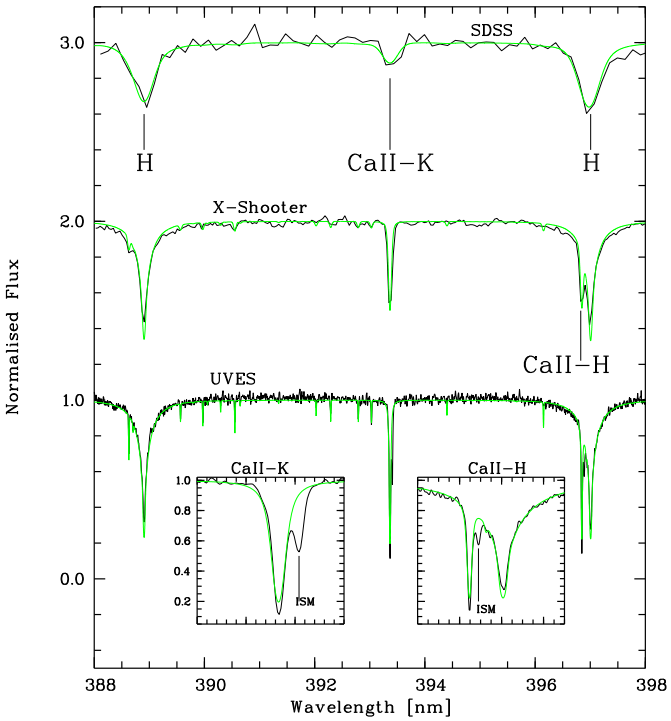

Fig. 13 The most metal-poor star currently known, SDSS J1029+1729. The figure shows the spectral range of the CaII K and K lines. A synthetic profile with metallicity 4.5 is superimposed, with α-enhanced by a factor of 2.5. This star has an iron abundance [Fe/H] = –4.89 and the absence of any measurable C or N enhancements indicates an overall metallicity of $Z < 7.4 \times 10^{-7}$. Adapted from Caffau et al. (2012).

Discoveries of stars with [Fe/H] as low as < -5 but strongly enhanced in carbon and nitrogen (e.g. Christlieb et al. 2002; Frebel et al. 2005) support this picture. Recently, Caffau et al. (2011, 2012, Fig. 13) reported the discovery of a low-mass star with the lowest overall metallicity yet known. Not only does it have one of the lowest iron abundances ([Fe/H] = –4.89), but the lack of carbon and nitrogen enhancement indicates that its metal-mass fraction $Z < 7.4 \times 10^{-7}$. Observations of such objects show that low-mass star formation is possible with extremely low metallicity and has a direct impact on our understanding of the first star formation at the highest redshift.

5 HISTORY OF REIONIZATION

The epoch of reionization is a crucial phase of cosmic evolution, when the UV photons from the first generation of galaxies and quasars ionized the neutral hydrogen in the IGM, ending the cosmic dark ages. Reionization is the most important radiative feedback from the first stars and galaxies, and represents the last major phase transition in cosmic history as neutral hydrogen in the Universe became ionized. With current observational constraints, it is still not clear (1) *When* did reionization happen? Whether it was early ($z \sim 15$) or late ($z \sim 6-8$), and whether it had an extended history or resembled a phase transition? (2) *How* did reionization proceed? Was it homogeneous or did it have a large scatter? How did HII regions grow during reionization and how did the overlap happen?

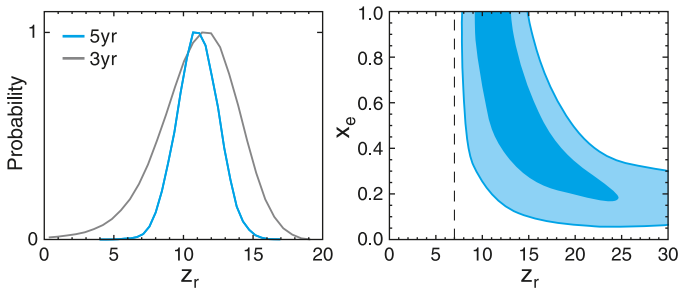

Fig. 14 *Left*: Marginalized probability distribution for $z_{\rm reion}$ in the standard model with instantaneous reionization. Sudden reionization at $z = 6$ is ruled out at a high level of significance, suggesting that reionization was a gradual process. *Right*: in a model with two steps of reionization (with ionization fraction x_e at redshift z_r, followed by full ionization at $z = 7$), the WMAP data are consistent with an extended reionization process. Adapted from Dunkley et al. (2009).

5.1 CMB Polarization

A key constraint on reionization comes from observations of polarizations in the CMB. Thomson scattering produces CMB polarization when free-electron scatterers are illuminated by an anisotropic photon distribution. Large scale CMB polarization therefore probes the ionization history by measuring the total optical depths of the CMB produced by free electrons generated from the reionization process. The strongest polarization constraint comes from the WMAP 7-yr results (Komatsu et al. 2011), with the best-fit values of $\tau = 0.088 \pm 0.014$ and $z_{\rm reion} = 10.6 \pm 1.2$, assuming an instantaneous reionization at $z_{\rm reion}$. However, the CMB polarization only measures an integrated reionization signal.

Figure 14 illustrates the degeneracy of the reionization redshift and detailed reionization history based on CMB data alone, using a simple reionization model assuming that the universe was partially reionized at $z_{\rm reion}$ to an ionization fraction of $x_{\rm e}$ and then became fully ionized at $z = 7$.

Detailed measurements of reionization history, therefore, require observations of high-redshift sources during the reionization era. These observations will not only map the evolution of the IGM ionization state, $f_{\rm HI}(z)$, but also reveal the topology and spatial distribution of the reionization process, and identify the sources that are responsible for reionization.

5.2 Gunn-Peterson Test

Gunn & Peterson (1965) first proposed using Lyα resonance absorption in the spectrum of distant quasars as a direct probe of the neutral hydrogen density in the IGM at high-redshift. The Gunn-Peterson optical depth for Lyα photons is

$$\tau_{\rm GP} = \frac{\pi e^2}{m_e c} f_\alpha \lambda_\alpha H^{-1}(z) n_{\rm HI}, \tag{2}$$

where f_α is the oscillator strength of the Lyα transition, λ_α = 1216 Å, $H(z)$ is the Hubble constant at redshift z, and $n_{\rm HI}$ is the density of neutral hydrogen in the IGM. At high redshifts

$$\tau_{\rm GP}(z) = 4.9 \times 10^5 \left(\frac{\Omega_m h^2}{0.13}\right)^{-1/2} \left(\frac{\Omega_b h^2}{0.02}\right) \left(\frac{1+z}{7}\right)^{3/2} \left(\frac{n_{\rm HI}}{n_{\rm H}}\right), \tag{3}$$

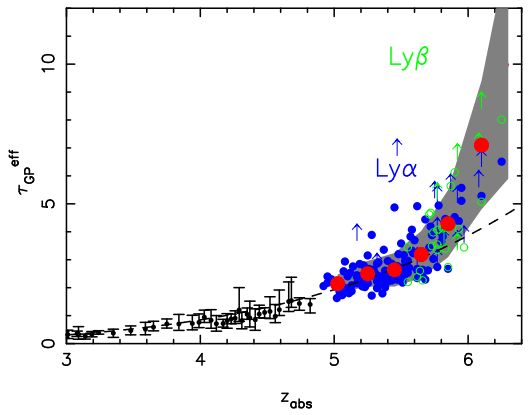

Fig. 15 Evolution of optical depth with combined Lyα and Lyβ results. The dashed line is for a redshift evolution of $\tau_{\rm GP} \propto (1+z)^{4.3}$. At $z > 5.5$, the best fit evolution has $\tau_{\rm GP} \propto (1+z)^{>10.9}$, indicating an accelerated evolution. The large open symbols with error bars are the average and standard deviation of optical depth at each redshift. The sample variance also increases rapidly with redshift. Adapted from Fan et al. (2006b).

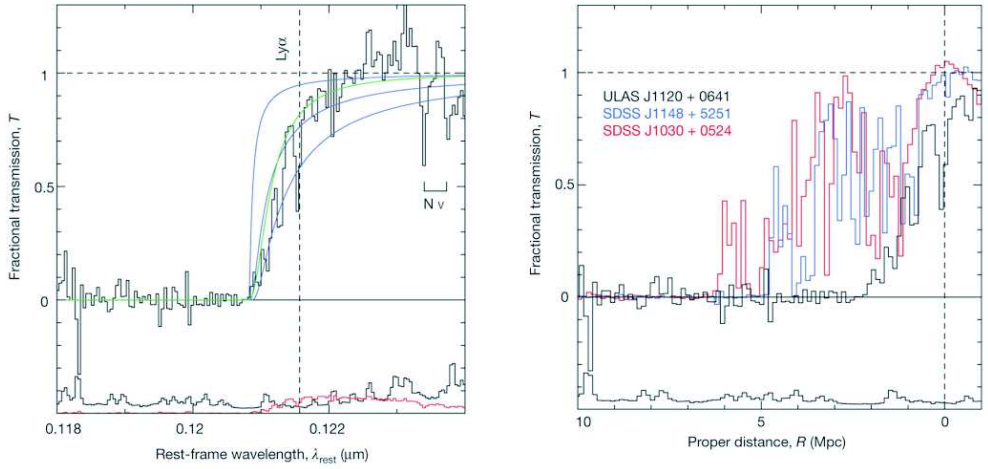

Fig. 16 Evidence for a significantly neutral IGM around the highest redshift quasar at $z = 7.1$. Left panel shows the excess absorption at the quasar rest-frame Lyα wavelength, likely due to the presence of a strong IGM Gunn-Peterson damping wing; right panel shows the very small near zone size of this $z = 7.1$ quasar compared with quasars at $z \sim 6$, indicating a much more neutral surrounding IGM. Both observations are consistent with an IGM neutral fraction of $f_{\rm HI} \geq 0.1$. Adapted from Mortlock et al. (2011).

for a uniform IGM. Even a tiny neutral fraction, $f_{\rm HI} \sim 10^{-4}$, gives rise to complete Gunn-Peterson absorption. Note that this test is only sensitive at the end of the reionization when the IGM is already mostly ionized, and saturates for the higher neutral fraction in the earlier stage.

Fan et al. (2006b) measured the evolution of Gunn-Peterson optical depths along the line of sight of 19 quasars with $z > 5.7$ from the SDSS (Fig. 15). They found that at $z_{\rm abs} < 5.5$, the optical depth can be best fitted as $\tau \propto (1+z)^{4.3}$, while at $z_{\rm abs} > 5.5$, the evolution of optical depth

accelerates: $\tau \propto (1+z)^{>10}$. There is also a rapid increase in the variation of optical depth along different lines of sight: $\sigma(\tau)/\tau$ increases from $\sim 15\%$ at $z \sim 5$, to $> 30\%$ at $z > 6$, in which τ is averaged over a scale of ~ 60 comoving Mpc. Assuming photoionization equilibrium and a model of IGM density distribution, one can convert the measured effective optical depth to IGM properties, such as the level of UV ionizing background and average neutral fraction. At $z > 6$ the volume-averaged neutral fraction of the IGM has increased to $> 10^{-3.5}$, with both ionizing background and neutral fraction experiencing about a one order of magnitude change over a narrow redshift range, and the mean-free-path of UV photons is shown to be < 1 physical Mpc at $z > 6$ (Fan et al. 2006b). However, with the emergence of complete Gunn-Peterson troughs at $z > 6$, it becomes increasingly difficult to place stringent limits on the optical depth and neutral fraction of the IGM. More sensitive tests are required to probe the ionization state of the IGM towards the neutral era.

5.3 Beyond the Gunn-Peterson Test: Evidence for a Significant Neutral Fraction at $z \sim 7$

For a largely neutral IGM, $\tau \sim 10^5$, the damping wing of the GP trough arising from the large GP optical depth of the neutral medium will extend into the red side of the Lyα emission line (Miralda-Escude 1998). This IGM damping is more extended than the absorption caused by a discrete high HI column density damped Lyα system and can be distinguished from it with high S/N spectroscopy. Using the spectrum of a GRB at $z = 6.3$, Totani et al. (2006) derived an upper limit of $f_{\rm HI} < 0.5$ based on the lack of an IGM damping wing.

The discovery of quasar ULAS J1120+0641($z = 7.085$) provides the first opportunity to study the IGM ionization state at $z \sim 7$. Mortlock et al. (2011, Figure 16) found that the Lyα emission line profile is quantitatively different from those of low-redshift quasars, and can only be fitted by assuming a smooth absorption envelop that extends to the red side of the rest-frame Lyα wavelength. This profile is difficult to explain by a damped system but can be easily modeled by an IGM with $f_{\rm HI} \sim 10$.

Luminous quasars produce a highly ionized HII region around them even when the IGM is still mostly neutral otherwise. The presence of (time bounded) cosmic Strömgren spheres around the highest redshift SDSS QSOs has been deduced from the observed difference between the redshift of the onset of the Gunn-Peterson effect and the systemic redshift of the host galaxy (White et al. 2005; Wyithe & Loeb 2004). The physical size of these spheres is typically ~ 5 Mpc at $z > 6$. The size of the Strömgren spheres is determined by the UV luminosity of the QSO, the HI density of the IGM, and the age of the QSO. However, the size of this HII region and the observed size of the proximity zone around quasars are both strongly affected by a number of factors, in particular, the details of radiative transfer inside the quasar's Strömgren sphere. In practice, it is also non-trivial to define the size of the proximity zone in the presence of patchy Lyα forest absorption.

Defining the size of a Strömgren sphere using quasar spectra is observationally difficult. Usually, one defines a *near zone* as the region close to the quasar along the line of sight in which photoionization is dominated by UV radiation from the quasar itself and the Gunn-Peterson optical depth is significantly lower than the general IGM. Fan et al. (2006b) studied the sizes of near zones associated with luminous SDSS quasars at $z > 5.7$, and found a decrease by a factor of 2.8 in the sizes of near zones from $z = 5.7$ to 6.4, validating the physical picture that quasar HII regions are expanding into an increasingly neutral IGM at higher redshifts. Since $\rm R_{NZ} \propto [(1+z) f_{HI}]^{-1/3}$, this corresponds to more than an order of magnitude increase in the IGM neutral fraction, consistent with Gunn-Peterson optical depth measurements over a similar redshift range.

A high S/N spectrum of ULAS J1120+0641 ($z = 7.085$) shows a deep Gunn-Peterson absorption trough from $z = 5.9$ to 7.0, although by itself, the limit on the IGM neutral fraction is similar to that at $z \sim 6$ due to saturation of the Gunn-Peterson effect. However, the absorption spectrum does show a significant difference from those of its $z \sim 6$ counterparts: as shown in Figure 16, the IGM optical depth remains high until very close to the quasar redshift, with a near zone size ~ 1.9

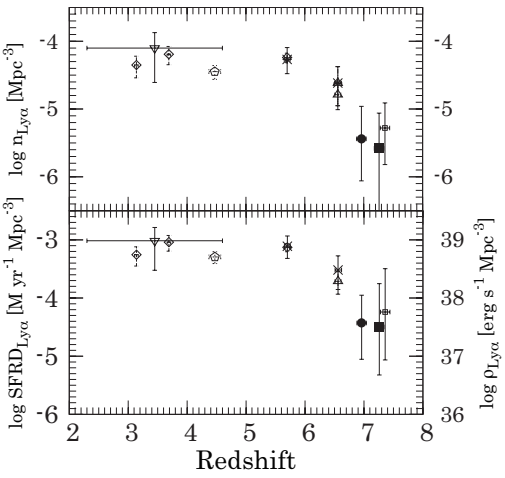

Fig. 17 Evolution of number density and star formation rate in Lyα galaxies at the end of reionization. A rapid decline in the density of Lyα galaxies is an indication that a partially neutral IGM is attenuating Lyα emission lines at $z \geq 6.5$. Adapted from Shibuya et al. (2012).

physical Mpc. This is a factor of ~ 2.5 smaller than the near zone size at $z \sim 6.2$, after correcting for the luminosity effect. After discussing other possible explanations, Mortlock et al. (2011) and Bolton et al. (2011) conclude that the small near zone size is consistent with an IGM neutral fraction $f_{\rm HI} \geq 0.1$, consistent with the damping wing result discussed above.

Properties of Lyα galaxies can also be used to directly probe the IGM neutral fraction. For $z \sim 6$, at ~ 10Å redward of Lyα of the host galaxy, the optical depth is of order unity for a neutral IGM. Without a large Strömgren sphere, the intrinsic Lyα emission will be considerably attenuated. In the simplest picture, one predicts: (1) the Lyα galaxy luminosity function will decrease sharply in an increasingly neutral IGM, even if the total star formation rate in the Universe remains roughly constant, and (2) the Lyα profiles will have a stronger red wing and a smaller average equivalent width before the onset of reionization.

Malhotra & Rhoads (2004) and Stern et al. (2005) combined the LALA survey of Lyα galaxies (Rhoads et al. 2003) with other Lyα surveys in the literature to determine the luminosity function of Lyα galaxies at $z = 6.5$ and 5.7. They found no evolution between these two redshift bins, consistent with the IGM being largely ionized by $z \sim 6.5$. However, using deep Subaru data, Ota et al. (2008) show a rapid decline of Lyα galaxy density at $z \sim 6.6 - 7.0$, but only a mild evolution in the density of continuum-selected galaxies over the same redshift range. The $z \sim 7.2$ Lyα emitter survey by Shibuya et al. (2012) confirmed this trend (Fig. 17). The extra density evolution can be interpreted as the attenuation due to a rapid evolution of neutral hydrogen fraction with $x_{\rm HI} \sim 0.3 - 0.6$ at $z \sim 7$. The interpretations of these results, however, require more detailed modeling (e.g Haiman 2002; Furlanetto et al. 2006; McQuinn et al. 2007).

Figure 18 shows the current limits on the cosmic neutral fraction versus redshift. The observations paint an interesting picture. On the one hand, studies of GP optical depths and variations suggest a qualitative change in the state of the IGM at $z \sim 6$. These data indicate a significant neutral fraction, $x_{\rm HI} > 10^{-3}$, and perhaps as high as 0.1, at $z \geq 6$, as compared to $x_{\rm HI} \leq 10^{-4}$ at $z < 5.5$. At $z \sim 7$, recent results using the quasar Lyα damping wing, near zone size and Lyα galaxy density confirm this trend, and suggest a significant neutral IGM with $f_{\rm HI} > 0.1$. The IGM characteristics at this epoch are consistent with the end of the 'percolation' stage of reionization (Gnedin &

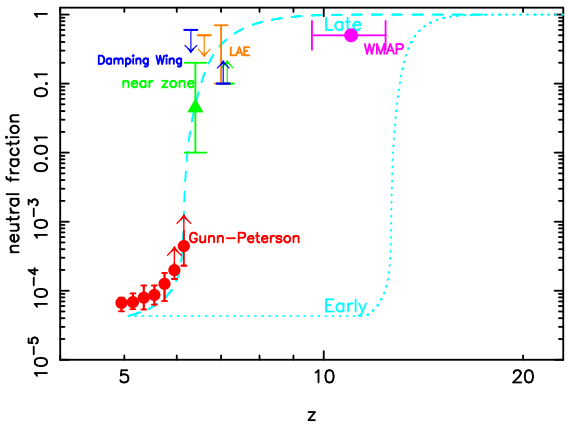

Fig. 18 The volume averaged neutral fraction of the IGM versus redshift using various techniques. The dashed line shows the model of Gnedin (2004) with late reionization at $z = 6-7$, and the dotted line illustrates the model with early reionization at $z \sim 14$. Current observational constraints indicate that the peak of the reionization activity is at $z \sim 7 - 13$. Although they still cannot differentiate between various models of reionization history, the results strongly suggest a gradual reionization process, which can only be confirmed with IGM observations at $z > 7$.

Fan 2006). On the other hand, the measurement of the large scale polarization of the CMB suggests a significant ionization fraction extending to higher redshifts, $z \sim 11 \pm 1$, implying a relatively early reionization.

Note that, however, the CMB results in Figure 18 assume a sharp "phase transition" in the IGM ionization state. The combination of the current constraints simply indicate that this "phase transition" picture is not consistent with observations; reionization is likely to be a prolonged, complex process. While there must have been a large amount of free electrons at $z \geq 10$ to explain the large CMB optical depth, the IGM remains only partially ionized until as late as $z \sim 7$. This result, if confirmed by future high-redshift observations, will have a significant impact on our understanding of the formation and evolution of the first generation galaxies.

6 FUTURE PROSPECTS

At the time of this review, the frontier for observing the distant Universe is at $z \sim 7$, at which secure spectroscopy of a handful of galaxies, quasars and GRBs exists, and detailed studies of both the intrinsic properties of galaxies and quasars, and the evolution of the IGM has started. At $z > 7$, samples of photometrically selected galaxies also begin to emerge, although detailed spectroscopy is still at, or beyond, the limit of the current generation facilities. Even though sample sizes are still small, at $z \sim 7$, or about 800 million years after the Big Bang, there is tentative evidence that the Universe is undergoing a fundamental transition as we are approaching the epoch of first light:

- A rapidly evolving galaxy population. As discussed in Section 2, the star formation density of the Universe begins to decrease significantly at $z > 6$. The galaxy density at $z \sim 7$ can barely keep the Universe ionized and a significantly higher fraction of escaping UV photons might be required, suggesting a change in intrinsic properties of galaxies.
- A rapidly evolving quasar population. As discussed in Section 3, the density of luminous quasars declines dramatically from $z \sim 2$ to 6. Meanwhile, growth of supermassive black holes begins to be severely limited by an accretion timescale at $z \geq 7$. Possible detection of dust-free quasars

from the metal-free environment is consistent with the overall picture that the first generation of supermassive black holes begins to emerge at this epoch.
– A rapidly evolving IGM. As discussed in Sections 4 and 5, current observations suggest that reionization has yet to be completed by $z \sim 6-7$, accompanied by a rapid increase in the neutral fraction of IGM. Furthermore, the IGM metal content appears to be evolving as well, suggesting the earliest IGM chemical enrichment process is not far behind.

WMAP results on CMB polarization give the most direct indication that the epoch of first generation star formation is at $z \geq 10$. In the coming decade, large, coordinated projects using current generation facilities, in particular deep HST surveys (e.g., CANDELS and CLASH) and deep spectroscopic observations on 8–10 m class telescopes, will continue to make progress on finding and studying physical processes in the population of galaxies at $z \sim 7-10$; Wide-field near-IR surveys using dedicated facilities such as VISTA will likely produce a handful of $z > 8$ quasars; the continued effort on follow-up of GRBs is also expected to extend both the range of redshifts and quality of GBR observations. However, direct observations of galaxies, quasars and IGM at $z > 10$ will likely have to await for the construction of the next generation of facilities. Indeed, studying the first light and reionization is both a major motivation and strong science requirement for many of these facilities being planned or under construction. Here we highlight a few examples:

– JWST: searching for the first light. JWST will represent order(s) of magnitude increase in the sensitivity of detecting and observing high-redshift galaxies and IGM, and will identify the reionization population. Figure 19 shows a prediction of high-redshift galaxy number counts as a function of limiting magnitudes. A JWST survey will reach an AB magnitude of 32, and detect dwarf galaxies at $z > 15$. A key project that surveys the HST/GOODS field will detect a large number of galaxies even up to $z \sim 15$. In addition, JWST/NIRSPEC will provide spectroscopic confirmation of at least the brighter candidates. These observations will provide the most valuable samples of high-redshift star-forming galaxies to probe the reionization history. Deep, space-based IR spectroscopy will allow studies of stellar population and star formation history of galaxy populations at $z > 7$ and will map the IGM ionization and enrichment history through high S/N spectroscopy of high-redshift quasars (and GRBs).
– EUCLID/WFIRST: search for the earliest supermassive black holes. Although the approved ESA mission EUCLID and the planned NASA mission WFIRST have their primary science goals in the area of dark energy, the wide-field near-infrared surveys these missions plan to carry out will reach $\sim 2-4$ magnitudes fainter than ground-based surveys with similar areal coverage, and will enable discoveries of a large number of the most distant quasars at $z > 8-10$, directly probing the epoch of formation and evolution of the first supermassive black holes. Both missions could find > 1000 quasars at $z > 7$ and ~ 20 quasars at $z > 10$ based on extrapolating current measurements of the quasar luminosity function at $z \sim 6$.
– 21cm: history of reionization. The 21cm transition of neutral hydrogen provides a unique probe of reionization, by directly observing the properties of IGM neutral hydrogen. The 21cm spin temperature begins to decouple from the CMB temperature as the Universe expands and first structures start to grow at high redshifts. Unlike the Lyα Gunn-Peterson effect, it does not saturate, and therefore can probe a mostly neutral IGM; unlike CMB polarization, it provides a full 3-dimensional map of the IGM structure and is sensitive to a wide range of astronomical scales and processes. Figure 20 presents a simulation of the 21cm signals over the first billion years of cosmic history. The key issue is the faintness of the 21cm signal and the removal of strong (and varying) foreground. A number of pathfinder facilities are close to completion and might allow statistical detections of high-redshift 21cm signals; the square kilometer array (SKA) will allow a full 3-D mapping of the cosmic evolution through 21cm radiation.

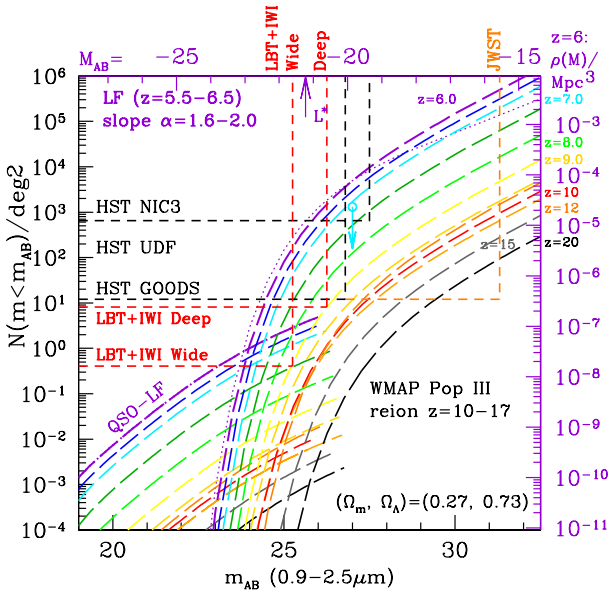

Fig. 19 Sensitivity of JWST deep surveys compared to the current generation HST surveys of high-redshift galaxies. JWST can trace the entire reionization epoch from the first light at $z \simeq 20$ to the end of reionization at $z \simeq 6$. Adapted from Windhorst et al. (2008).

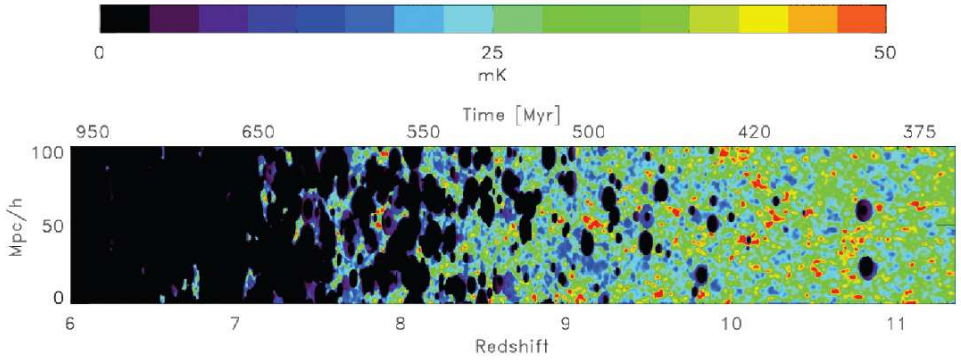

Fig. 20 Simulation of 21cm signals as a probe of reionization. The figure shows a slice through redshift as reionization proceeds in the IGM. Note the small expected signal compared to the strong foreground radiation. Adapted from Thomas et al. (2009).

Acknowledgements I would like to thank the Kavli Institute of Astronomy and Astrophysics, Peking University, for their hospitality. I am also grateful for long term collaborations with many colleagues on the studies of high-redshift quasars, galaxies and reionization, in particular Bob Becker, Zheng Cai, Chris Carilli, Linhua Jiang, Ian McGreer, Gordon Richards, Don Schneider, Michael Strauss, Marianne Vestergaard, Ran Wang, Fabian Walter, Rick White and Haojing Yan. My research has been supported by a David and Lucile Packard Fellowship, and the US National Science Foundation (NSF) Grants AST 08-06861 and AST 11-07682.

References

Abel, T., Bryan, G. L., & Norman, M. L. 2002, Science, 295, 93
Adelberger, K. L., Shapley, A. E., Steidel, C. C., et al. 2005, ApJ, 629, 636
Becker, R. H. et al. 2001, AJ, 122, 2850
Becker, G. D., Sargent, W. L. W., Rauch, M., & Calverley, A. P. 2011, ApJ, 735, 93
Becker, G. D., Sargent, W. L. W., Rauch, M., & Simcoe, R. A. 2006, ApJ, 640, 69
Bertoldi, F., Carilli, C. L., Cox, P., et al. 2003, A&A, 406, L55
Blain, A. W., Frayer, D. T., Bock, J. J., & Scoville, N. Z. 2000, MNRAS, 313, 559
Bolton, J. S., et al. 2011, MNRAS, 416, L70
Bouwens, R. J., Illingworth, G. D., Labbe, I., et al. 2011a, Nature, 469, 504
Bouwens, R. J., Illingworth, G. D., Oesch, P. A., et al. 2011b, ApJ, 737, 90
Bowler, R. A. A., Dunlop, J. S., McLure, R. J., et al. 2012, arXiv:1205.4270
Boyle, B. J., Shanks, T., Croom, S. M., et al. 2000, MNRAS, 317, 1014
Bromm, V., & Loeb, A. 2003, Nature, 425, 812
Bromm, V., & Larson, R. B. 2004, ARA&A, 42, 79
Bromm, V., & Yoshida, N. 2011, ARA&A, 49, 373
Bromm, V., Yoshida, N., & Hernquist, L. 2003, ApJ, 596, L135
Bunker, A. J., Stanway, E. R., Ellis, R. S., & McMahon, R. G. 2004, MNRAS, 355, 374
Caffau, E., Bonifacio, P., François, P., et al. 2011, Nature, 477, 67
Caffau, E., Bonifacio, P., François, P., et al. 2012, A&A, 542, A51
Cai, Z., Fan, X., Jiang, L., et al. 2011, ApJ, 736, L28
Dave, R., Finlator, K., & Oppenheimer, B, D., 2006, MNRAS 370, 273
Christlieb, N., Bessell, M. S., Beers, T. C., et al. 2002, Nature, 419, 904
Ciardi, B., & Ferrara, A. 2005, Space Sci. Rev., 116, 625
Ciardi, B., & Loeb, A. 2000, ApJ, 540, 687
Dietrich, M. et al. 2003, ApJ, 596, 817
Clément, B., Cuby, J.-G., Courbin, F., et al. 2012, A&A, 538, A66
Cuby, J.-G., Hibon, P., Lidman, C., et al. 2007, A&A, 461, 911
Cucchiara, A., Levan, A. J., Fox, D. B., et al. 2011, ApJ, 736, 7
Dawson, S., Rhoads, J. E., Malhotra, S., et al. 2004, ApJ, 617, 707
De Rosa, G., Decarli, R., Walter, F., et al. 2011, ApJ, 739, 56
Djorgovski, S. G., Castro, S., Stern, D., & Mahabal, A. A. 2001, ApJ, 560, L5
Dunkley, J., Komatsu, E., Nolta, M. R., et al. 2009, ApJS, 180, 306
Dunlop, J. S. 2012, in The First Galaxies - Theoretical Predictions and Observational Clues, eds. V. Bromm, B. Mobasher, & T. Wiklind (Springer) (arXiv:1205.1543)
Fan, X., Strauss, M. A., Schneider, D. P., et al. 2001, AJ, 121, 54
Fan, X., Hennawi, J. F., Richards, G. T., et al. 2004, AJ, 128, 515
Fan, X., Strauss, M. A., Becker, R. H., et al. 2006a, AJ, 132, 117
Fan, X., Carilli, C. L., & Keating, B. 2006b, ARA&A, 44, 415
Fan, X., Strauss, M. A., Richards, G. T., et al. 2006c, AJ, 131, 1203
Finkelstein, S. L., Papovich, C., Ryan, R. E., Jr., et al. 2012, arXiv:1206.0735
Finlator, K., Davé, R., & Özel, F. 2011, ApJ, 743, 169
Frebel, A., Aoki, W., Christlieb, N., et al. 2005, Nature, 434, 871
Freudling, W., Corbin, M. R., & Korista, K. T. 2003, ApJ, 587, L67
Furlanetto, S. R., & Loeb, A. 2003, ApJ, 588, 18
Furlanetto, S. R., Zaldarriaga, M., & Hernquist, L. 2006, MNRAS, 365, 1012
Gehrels, N., Chincarini, G., Giommi, P., et al. 2004, ApJ, 611, 1005
Gnedin, N. Y. 2004, ApJ, 610, 9

Gnedin, N. Y. 2008, ApJ, 673, L1
Gnedin, N. Y., & Fan, X. 2006, ApJ, 648, 1
Gonzalo Diaz, C., Ryan-Weber, E. V., Cooke, J., et al. 2011, arXiv:1104.4194 (MNRAS accepted)
Grogin, N. A., Kocevski, D. D., Faber, S. M., et al. 2011, ApJS, 197, 35
Gunn, J. E., & Peterson, B. A. 1965, ApJ, 142, 1633
Haiman, Z. 2002, ApJ, 576, L1
Hu, E. M., Cowie, L. L., McMahon, R. G., et al. 2002, ApJ, 568, L75
Iliev, I. T., Mellema, G., Pen, U.-L., et al. 2006, MNRAS, 369, 1625
Iye, M. 2008, in Society of Photo-Optical Instrumentation Engineers (SPIE) Conference Series, Observatory Operations: Strategies, Processes, and Systems II, eds. R. J. Brissenden, & D. R. Silva, 7016, 701602
Iye, M., Ota, K., Kashikawa, N., et al. 2006, Nature, 443, 186
Jiang, L., Fan, X., Vestergaard, M., et al. 2007, AJ, 134, 1150
Jiang, L., Fan, X., Bian, F., et al. 2009, AJ, 138, 305
Jiang, L., Fan, X., Brandt, W. N., et al. 2010, Nature, 464, 380
Kashikawa, N. et al. 2006, ApJ, 648, 7
Koekemoer, A. M., Faber, S. M., Ferguson, H. C., et al. 2011, ApJS, 197, 36
Komatsu, E., Smith, K. M., Dunkley, J., et al. 2011, ApJS, 192, 18
Loeb, A., & Barkana, R. 2001, ARA&A, 39, 19
Mackey, J., Bromm, V., & Hernquist, L. 2003, ApJ, 586, 1
Madau, P., Ferrara, A., & Rees, M. J. 2001, ApJ, 555, 92
Maiolino, R., Gallerani, S., Neri, R., et al. 2012, arXiv:1204.2904 (MNRAS, in press)
Malhotra, S., & Rhoads, J. E. 2004, ApJ, 617, L5
McQuinn, M., Hernquist, L., Zaldarriaga, M., & Dutta, S. 2007, MNRAS, 381, 75
Miralda-Escude, J. 1998, ApJ, 501, 15
Miralda-Escudé, J., Haehnelt, M., & Rees, M. J. 2000, ApJ, 530, 1
Morales, M. F., & Wyithe, J. S. B. 2010, ARA&A, 48, 127
Mortlock, D. J., Patel, M., Warren, S. J., et al. 2009, A&A, 505, 97
Mortlock, D. J., Warren, S. J., Venemans, B. P., et al. 2011, Nature, 474, 616
Loeb, A., 2010, How did the First Stars and Galaxies Form (Princeton Univ. Press)
Nagao, T., Motohara, K., Maiolino, R., et al. 2005, ApJ, 631, L5
Oh, S. P. 2002, MNRAS, 336, 1021
Ota, K., Iye, M., Kashikawa, N., et al. 2008, ApJ, 677, 12
Ouchi, M. et al. 2010, ApJ, 723, 869
Ouchi, M., Shimasaku, K., Akiyama, M., et al. 2008, ApJS, 176, 301
Pettini, M., Madau, P., Bolte, M., et al. 2003, ApJ, 594, 695
Postman, M., Coe, D., Benítez, N., et al. 2012, ApJS, 199, 25
Rees, M. J. 1998, in Proceedings of the National Academy of Sciences Colloquium: The Age of the Universe, Dark Matter, and Structure Formation (NAS: Washington DC), 47
Rhoads, J. E., Dey, A., Malhotra, S., et al. 2003, AJ, 125, 1006
Riechers, D. A., Walter, F., Carilli, C. L., Bertoldi, F., & Momjian, E. 2008, ApJ, 686, L9
Riechers, D. A., Walter, F., Carilli, C. L., & Lewis, G. F. 2009, ApJ, 690, 463
Riechers, D. A., Capak, P. L., Carilli, C. L., et al. 2010, ApJ, 720, L131
Robertson, B. E., & Ellis, R. S. 2012, ApJ, 744, 95
Robertson, B. E., Ellis, R. S., Dunlop, J. S., McLure, R. J., & Stark, D. P. 2010, Nature, 468, 49
Ryan-Weber, E. V., Pettini, M., Madau, P., & Zych, B. J. 2009, MNRAS, 395, 1476
Salvaterra, R., Della Valle, M., Campana, S., et al. 2009, Nature, 461, 1258
Schaye, J., Aguirre, A., Kim, T.-S., et al. 2003, ApJ, 596, 768
Schmidt, M., Schneider, D. P., & Gunn, J. E. 1995, AJ, 110, 68

Schneider, R., Ferrara, A., Salvaterra, R., Omukai, K., & Bromm, V. 2003, Nature, 422, 869
Shapley, A. E., Steidel, C. C., Pettini, M., Adelberger, K. L., & Erb, D. K. 2006, ApJ, 651, 688
Shibuya, T., Kashikawa, N., Ota, K., et al. 2012, ApJ, 752, 114
Siana, B., Teplitz, H. I., Colbert, J., et al. 2007, ApJ, 668, 62
Simcoe, R. A., Cooksey, K. L., Matejek, M., et al. 2011, ApJ, 743, 21
Songaila, A. 2001, ApJ, 561, L153
Stark, D. P., Ellis, R. S., Richard, J., et al. 2007, ApJ, 663, 10
Steidel, C. C., Giavalisco, M., Pettini, M., Dickinson, M., & Adelberger, K. L. 1996, ApJ, 462, L17
Steidel, C. C., Pettini, M., & Adelberger, K. L. 2001, ApJ, 546, 665
Stern, D., Yost, S. A., Eckart, M. E., et al. 2005, ApJ, 619, 12
Taniguchi, Y., Shioya, Y., & Trump, J. R. 2010, ApJ, 724, 1480
Tanvir, N. R., Fox, D. B., Levan, A. J., et al. 2009, Nature, 461, 1254
Thomas, R. M., Zaroubi, S., Ciardi, B., et al. 2009, MNRAS, 393, 32
Totani, T., Kawai, N., Kosugi, G., et al. 2006, PASJ, 58, 485
Vanzella, E., Pentericci, L., Fontana, A., et al. 2011, ApJ, 730, L35
Venemans, B. P., McMahon, R. G., Walter, F., et al. 2012, ApJ, 751, L25
Volonteri, M. 2010, A&A Rev., 18, 279
Walter, F., Carilli, C., Bertoldi, F., et al. 2004, ApJ, 615, L17
Walter, F., Decarli, R., Carilli, C., et al. 2012, Nature, 486, 233
Wang, R., Carilli, C. L., Beelen, A., et al. 2007, AJ, 134, 617
Wang, R., Carilli, C. L., Wagg, J., et al. 2008, ApJ, 687, 848
Wang, R., Carilli, C. L., Neri, R., et al. 2010, ApJ, 714, 699
Warren, S. J., Hewett, P. C., Irwin, M. J., & Osmer, P. S. 1987, Nature, 330, 453
Whalen, D., O'Shea, B. W., Smidt, J., & Norman, M. L. 2008, ApJ, 679, 925
White, R. L., Becker, R. H., Fan, X., & Strauss, M. A. 2005, AJ, 129, 2102
Willott, C. J., Delorme, P., Reylé, C., et al. 2010a, AJ, 139, 906
Willott, C. J., Albert, L., Arzoumanian, D., et al. 2010b, AJ, 140, 546
Windhorst, R. A., Hathi, N. P., Cohen, S. H., et al. 2008, Advances in Space Research, 41, 1965
Wyithe, J. S. B., & Loeb, A. 2004, Nature, 432, 194
Yan, H., & Windhorst, R. A. 2004, ApJ, 612, L93
Yoshida, N., Omukai, K., Hernquist, L., & Abel, T. 2006, ApJ, 652, 6
Zackrisson, E. 2012, arXiv:1206.5806
Zheng, W., Postman, M., Zitrin, A., et al. 2012, arXiv:1204.2305
Zheng, Z., Cen, R., Trac, H., & Miralda-Escudé, J. 2010, ApJ, 716, 574